

Final Draft
of the original manuscript:

Merckelbach, L.:

**On the probability of underwater glider loss due to collision
with a ship**

In: Journal of Marine Science and Technology (2012) Springer

DOI: 10.1007/s00773-012-0189-7

On the probability of glider loss due to collision with ships

Lucas Merckelbach

Received: date / Accepted: date

Abstract The demonstrated fitness as a measurement platform for the open ocean has sparked a growing interest to operate underwater gliders also in shallow coastal areas. In this environment gliders face additional challenges such as strong (tidal) currents and high shipping intensity. This work focuses on the probability of losing a glider resulting from a collision with a ship. A ship density map is constructed for the German Bight from observed ship movements from Automatic Identification System (AIS) data. A simple probability model is developed to interpret ship densities in terms of collision probabilities. More realistic, but also more computationally expensive Monte-Carlo simulations were carried out for verification. The model can be used to generate geographic maps showing the probability of glider loss due to collisions. Such maps can serve as an aid in planning glider missions.

Keywords gliders · collision · AIS · German Bight

1 Introduction

Underwater gliders, or gliders for short, are buoyancy-engine propelled autonomous underwater vehicles (AUVs): they can attain positive or negative buoyancy to climb or sink, respectively. Being a torpedo-like shape of about 1.5 m in length and equipped with wings, vertical motion leads to a horizontal velocity, enabling a glider to traverse the oceans in a saw-tooth way down to depths of 1000-1500 m. When at the surface, gliders use global positioning system (GPS) for navigation and two-way satellite communication systems, allowing them to be controlled from shore. Davis *et al.* [1] give an in-depth account of the principles of operation.

Lucas Merckelbach
Max Planck Str. 1 D21501 Geesthacht, Germany
Tel.: +49-4152-871515
Fax: +49-4152-871550
E-mail: lucas.merckelbach@hzg.de

Gliders have been mostly utilised in oceanic and off-shore experiments [11]. Operating in oceans, gliders have shown to excel at surveying for long periods on end, *i.e.* order of months. Furthermore, the operational costs compared to shipborne observations are significantly lower [11]. Therefore, it should be no surprise that gliders are becoming increasingly more popular as measurement platforms in ocean observatories. Operating gliders in coastal environment (coastal observatories) has not been as wide spread yet, as gliders face additional challenges specific to coastal waters. However, the demonstrated fitness of gliders for use in the open ocean has sparked the interest to operate gliders in coastal observatories too.

One of such coastal observatories is being built in the framework of the Cosyna project (Coastal Observation System for Northern and Arctic Seas). This project aims at the “Development and test of analysis systems for the operational synoptic description of the environmental status of the North Sea and of Arctic coastal waters.”¹ In practice, the main focus of the Cosyna observatory is the German Bight, *i.e.* the German part of the North Sea, which is characterised by shallow waters ($\approx 30 - 40$ m), strong tidal currents ($\approx 0.5 - 1$ m/s) and intensive (commercial) shipping to and from the harbours of Hamburg, Willemshaven and Cuxhaven. In addition to operational costs, the risk of losing a glider during a mission should be considered as well, when evaluating the fitness of gliders in a coastal observatory such as Cosyna.

The loss of a glider can have many different reasons. With most gliders being deployed far off-shore and in oceans, it is most likely that a glider gets into trouble due to failing hardware or software and possibly due to a collision with a ship during (an emergency) recovery. In coastal waters, however, a glider faces other risks in addition those mentioned. Currents in coastal waters, both tidal and density driven (due to river outflow), can be so strong that they limit or even inhibit the maneuverability of gliders. In addition, fresh water outflow due to rivers can cause large salinity and density gradients, limiting the positive or negative buoyancy compensation by the glider’s buoyancy engine. In addition to these “environmental” risks, coastal water impose an increased risk on glider loss due to a collision with a ship, as coastal waters are often characterised by extensive shipping. The aim of the present paper is to quantify the risk of a glider operation with respect to ship-glider collisions.

Due to the relative recent appearance of the glider platform in coastal areas, the topic of ship-glider collisions has not received much attention. In the marine biology discipline the collision between ships and whales has been the subject of several studies [5][7][12]. However, these studies report mainly focus on reports and statistics of injuries and casualties inflicted upon whales. Laist *et al.* [7] and Van der Laan [12] also mention a relationship between ship speed and how likely it is that a collision between whale and ship will be fatal. Van der Laan [12] supports this with a model based on a random walk model described by Gallos and Argyrakis [3]. In this model, a domain of finite size is considered, stationary with respect to the ship, and the whale performs a random walk. The duration of the random walk is taken equal to the time the ship requires to traverse the domain. From this, the probability that the whale and ship collide is calculated as function of the ship’s speed. The random walk

¹ <http://www.cosyna.de>, accessed 1 July 2011.

assumption does not hold for the case where a glider follows a certain transect amidst passing ships.

The modelling of ship-ship collisions, on the other hand, has received more attention, see [4] and references therein. Older approaches assume a so-called static collision model, in that ships are assumed not to take evasive actions when on collision course. The probability of collision is calculated as the product of the probability of ships encountering – *i.e.* two ships are a collision course – and the probability to take proper evasive actions due to technical problems or human error [2][8]. More recent studies include a dynamical collision model in which the extent to which evasive measures can be taken, are explicitly accounted for [4]. The introduction of the Automatic Identification System (AIS), which are messages transmitted between ships, and ship and shore over HighFrequency radio channels, to make ships “visible” to each other, has opened a new avenue for research. These messages contain, amongst other things, information on position, speed and ship dimensions. These signals can be picked up by shore stations and the information fed to databases. Mining these databases facilitates in simulating ship traffic realistically [9][10]. In the case of ship-glider collisions, both the ship and glider are oblivious to one another, so that a (simpler) static collision model [2][8] is therefore more appropriate to be applied than a dynamic collision model.

This paper builds upon several ideas taken from the ship-ship collision research. The aim is to develop a method to quantify the probability of a ship-glider collision and to apply the method to the area relevant in the Cosyna framework, namely the German Bight. To this end, a simple probability model is developed that, based on maps of ship density, calculates the probability of a collision for a given transect or mission. Ship density data were obtained from a website that presents live positions of ships based on emitted Automatic Identification System (AIS) signals that are received by various stations along coasts. For verification purposes, a Monte-Carlo simulation is setup. Both methods are applied to two glider transects in the German bight, one of which crosses several busy shipping lanes.

2 Ship traffic data

The Marine Traffic project website is part of an academic, open, community-based project and hosted by the Department of Product and Systems Design Engineering, University of the Aegean, Greece. The website is dedicated to collect and present data which are exploited in many marine and naval research areas, see <http://www.marinetraffic.com/ais/faq.aspx>². Ship positions are collected from partners of the Marine Traffic project who have set up AIS receivers and feed their information into a central database. The Marine Traffic’s website <http://www.marinetraffic.com/ais/> presents the near-real time ship positions based on the information of the central database.

A Python script was developed to download ship positions for the area (53.5N,5.5E)-(54.5N,9.5E), collecting data at 5 minute intervals for the month July 2010. Permission to use these data was kindly granted by D. Lekkas (Department of Product and Systems Design Engineering University of the Aegean, Greece).

² Accessed on 13 January 2011.

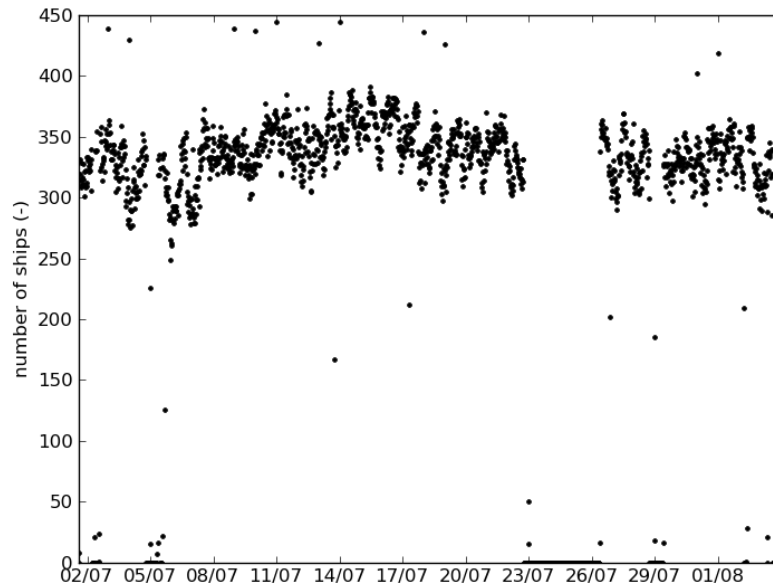


Fig. 1 Number of ships observed per 30 minute interval.

Figures 1 and 2 show the number of ships collected per 30 minute interval as function of time and the number of ships collected per 30 minute interval as function of the time of day, respectively. It is seen that on average 300-350 ships are in the area. During the month July, changes in intensity of traffic are modest, whereas the traffic is only slightly more intense during mid-day and early evening. Around 5, 23-26 and 29 July network issues caused the data collection to fail.

A box-counting method with box sizes of $1 \times 1 \text{ km}^2$ yields the averaged number of ships per box per hour for this month, as shown in Figure 3. The contours of shipping lanes connecting the harbours of Hamburg, Wilhelmshaven, and Bremen are clearly visible.

From Figure 3 it is clear that some areas are best to be avoided by gliders. But, how likely is it to lose a glider as a result of a collision with a ship?

To answer this question we consider two transects, originating from Helgoland. One transect is due South and crosses the main shipping lane to and from the harbour of Hamburg. The other transect is due East and finds itself in an area with less intense shipping traffic. These transects are indicated by the white dotted lines in Figure 3 and have the latitude/longitude coordinates $(54.245, 7.790) - (52.837, 7.790)$ and $(54.245, 7.790) - (54.245, 8.400)$, respectively. The selected transects cover high and low intensity shipping traffic, and are of scientific interest with respect to tracer budget calculations along the coast.

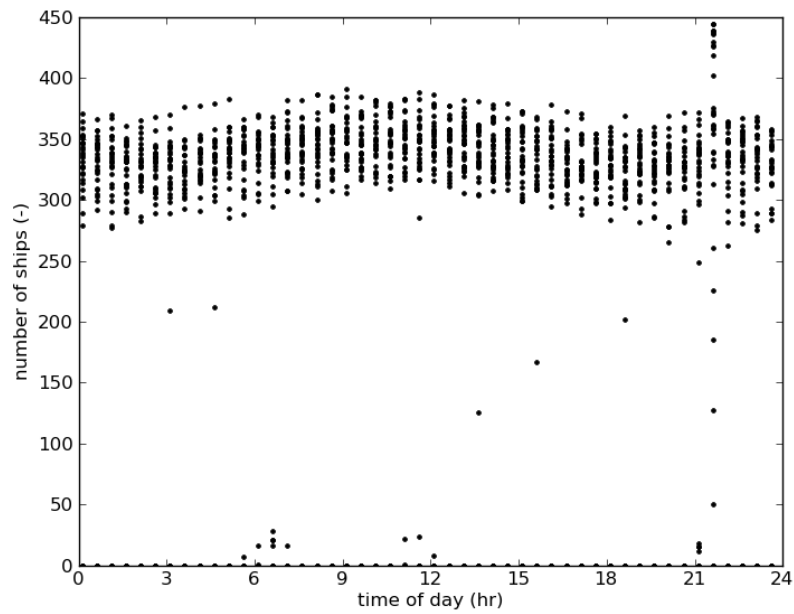


Fig. 2 Number of ships observed as function of the hour of day.

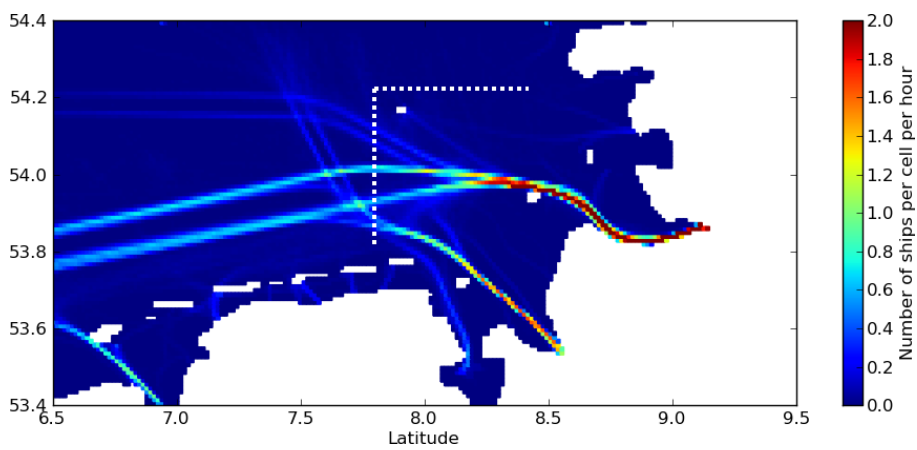


Fig. 3 Ship density in the German Bight area for July 2010. The dotted white lines indicate the EW and NS glider transects used in this study.

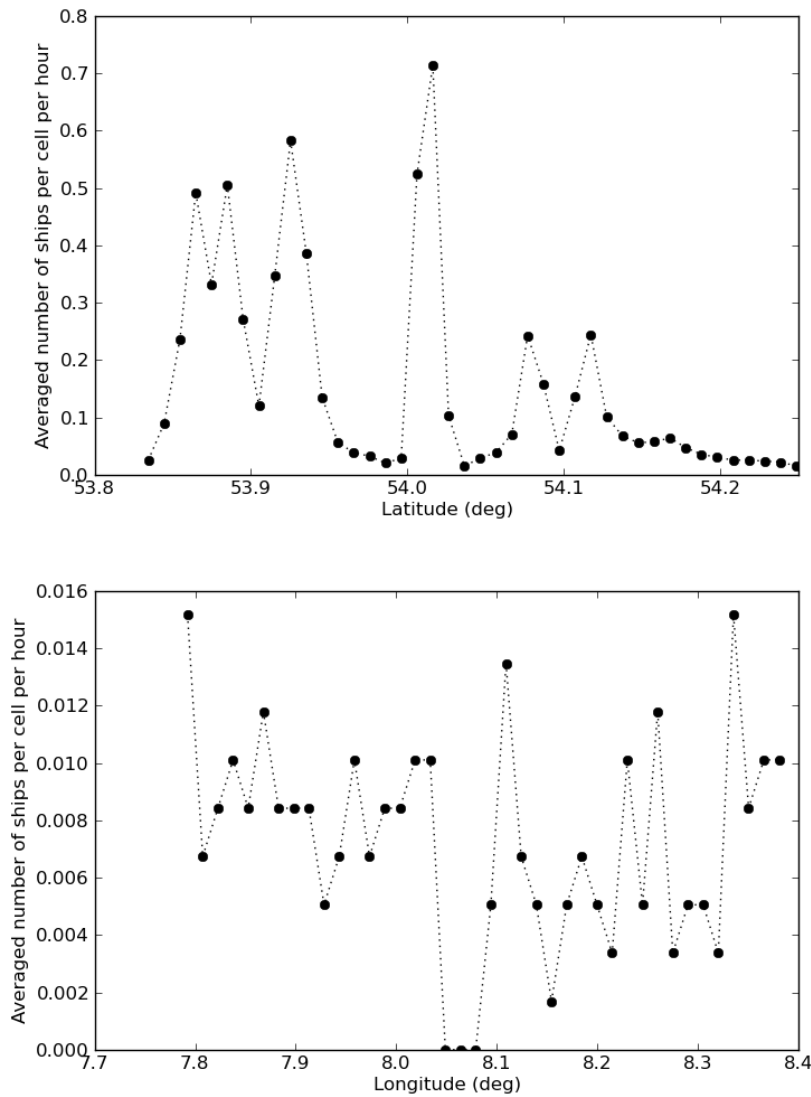


Fig. 4 The averaged number of ships per 1x1 km² cell per hour for the North-South transect (upper panel) and the East-West transect (lower panel).

Figure 4 shows the number of ships found per hour per 1x1 km² cells along the North-South (NS) and East-West (EW) transects, respectively. The NS transect show regions with high ship density corresponding to the shipping lanes that can be observed in Figure 3. The average ship density, $\bar{\rho}_s$, is about 0.16 ships per cell per

hour. The shipping density for the EW transect is substantially lower, amounting to an average shipping density of about 0.007 ships per cell per hour.

3 Probability on collision

To estimate the chance a glider has in order to make a successful transect crossing, *i.e.* not colliding with a ship, we consider the scenario where the glider crosses a squared cell with size L_t , travelling North at speed v_g , and a ship crossing the same cell, travelling East at speed v_s . The ship's length and width are denoted by L and B , respectively. For a collision to occur, there must be a ship in the cell, the ship track and glider track must intersect, and the glider must be the ship's path. Normally, a ship travels (much) faster than the glider, so that, for a cell that contains both a glider and a ship, it can be assumed that if $v_s \gg v_g$, the ship's and glider's tracks intersect at some time during the glider's transit. The transit time, $T_t = L_t/v_g$, is the time the glider requires to cross the cell. Then, the probability for the glider to collide with a ship while crossing a cell is given by

$$p_c = \rho T_t \times \frac{B}{L_t} \times \psi, \quad (1)$$

where $\rho_s T_t$ is the probability that a ship is present in the cell (and implicitly the probability that the ship's and glider's tracks intersect), and B/L_t the probability that the glider is in the path of the ship, given that the tracks intersect, and ψ the probability that the glider is not deep enough to avoid a collision with the ship by gliding underneath.

The probability that the glider survives a mission, \tilde{p}_m , is equal to the probability that the glider does not collide with a ship during any of the cell crossings. Therefore,

$$\tilde{p}_m = (1 - p_c)^n, \quad (2)$$

where n is the total number of cells to be traversed during the planned mission.

Note that it is implicitly assumed that every ship that is observed within a cell together with a glider, crosses the glider transect. This is not true for moored ships, or very slow moving ships. Neglecting the probability of a failing glider as a result of a collision with a moored ship, ships with a reported speed of less than 0.5 knots (≈ 1 km/hr) are excluded from further analysis.

3.1 Displacement hulls

By far most ships that the glider may encounter have displacement hulls. This means that at the bow of a moving ship the water is displaced to either side of the ship and accelerated. A (floating) glider that is in the water in front of the bow, will be advected by the accelerating water. However, due to the inertia of the glider the path the glider will follow will generally be different from the streamlines. Although the streamlines will all go around the ship, the glider may collide and sucked into the

ship's propellers, which is assumed to be fatal for the glider. In this section the accelerating flow around the bow is modelled as a potential flow. Assumptions implicitly made are that the flow is incompressible, irrotational and inviscid. In the ship's wake significant energy loss due to turbulence occurs and here the flow around the ship will significantly be different for potential flow. It is assumed that if the glider is advected alongside the ship's hull from bow to mid-ship with a minimum distance to the hull greater than a safety distance δ , the glider will never collide with the ship. Therefore, we consider here the bow only.

3.2 Potential flow around a ship

The shape of the horizontal cross-section of the ship is modelled as an ellipse with a transverse radius of $L/2$ and a conjugate radius of $B/2$. This allows the ship's shape to be linearly transformed to a circle, so that the problem of 2D planar potential flow around the ship reduces to potential flow around a cylinder. A definition sketch is shown in Figure 5. Herein ξ and η define the non-dimensional coordinate system relative to the centre of the cylinder. The streamlines are given [6, for example]

$$\Psi = u\eta - \frac{\mu\eta}{\xi^2 + \eta^2}, \quad (3)$$

where u and μ are non-dimensional coefficients. The non-dimensional velocities u_ξ and u_η are given by

$$u_\xi = \frac{\partial\Psi}{\partial\eta} \quad ; \quad u_\eta = -\frac{\partial\Psi}{\partial\xi}, \quad (4)$$

giving

$$u_\xi = u - \mu \frac{\xi^2 - \eta^2}{(\xi^2 + \eta^2)^2} \quad (5)$$

$$u_\eta = -2\mu \frac{\xi\eta}{(\xi^2 + \eta^2)^2}. \quad (6)$$

At the stagnation point S with coordinates $\xi = -1$ and $\eta = 0$, the velocity $u_\xi = 0$, so that $u = \mu$.

Introducing the (dimensional) coordinates x and y

$$x = \frac{L}{2}\xi \quad ; \quad y = \frac{B}{2}\eta, \quad (7)$$

we get

$$u_x = \frac{\partial\Psi}{\partial\eta} \frac{\partial\eta}{\partial y} = 2u_\xi/B \quad (8)$$

$$u_y = -\frac{\partial\Psi}{\partial\xi} \frac{\partial\xi}{\partial x} = 2u_\eta/L. \quad (9)$$

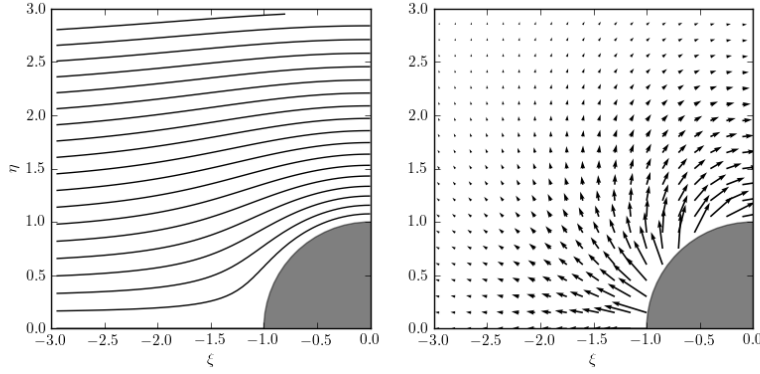


Fig. 5 Potential flow around a (quarter of a) cylinder with radius 1. The left-hand panel shows the streamlines (going from left to right), whereas the right-hand panel shows the vector field reduced by u_s , i.e. the flow field that forces the glider.

The undisturbed velocity is given by $(u_s, 0)^T$, where u_s is the speed of the ship, so that

$$u_x = u_s - u_s \frac{\xi^2 - \eta^2}{(\xi^2 + \eta^2)^2} \quad (10)$$

$$u_y = -2u_s \frac{B}{L} \frac{\xi \eta}{(\xi^2 + \eta^2)^2}. \quad (11)$$

3.3 Glider model and results

With respect to the ship, the glider initially moves towards the ship at a speed equal to the ship. If the glider's speed (relative to the ship) differs from the local current vector $u = (u_x, u_y)^T$, a drag force is generated that will accelerate the glider. The glider is modelled as a point object. Furthermore, the speed of the glider in an earth-referenced coordinate frame is taken equal to zero, as it is assumed that the glider speed is much smaller than the ship's. The dynamics of the glider is modelled as

$$(m + m_a) \dot{v} = \frac{1}{2} \rho C_d A V^2 e_v, \quad (12)$$

where m is the mass of the glider, m_a the added mass, ρ the density of the water, C_d the drag coefficient based on the frontal area A , V the magnitude of the velocity difference $u - v$, which has the direction given by the unity vector e_v . The velocity of the glider v relates to its position x_g as $\dot{x}_g = v$. Although the orientation of the glider with respect to the direction of u is not explicitly taken into account, it is taken into account by the settings of the parameters C_d and A .

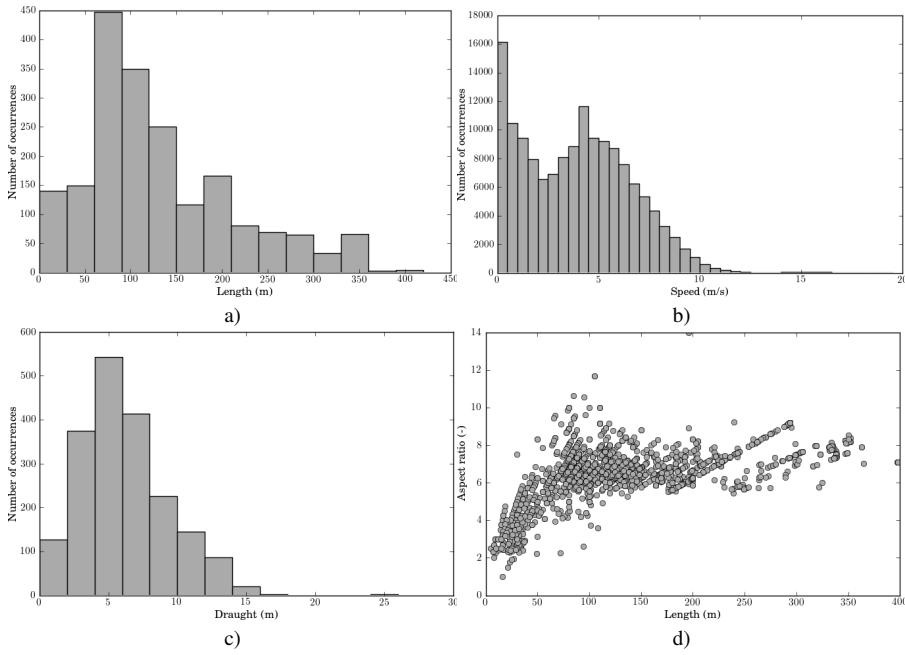


Fig. 6 Histograms of observed ship length (panel a), ship speed (panel b) and ship draught (panel c), and aspect ratio (L/B) as function of ship length (panel d).

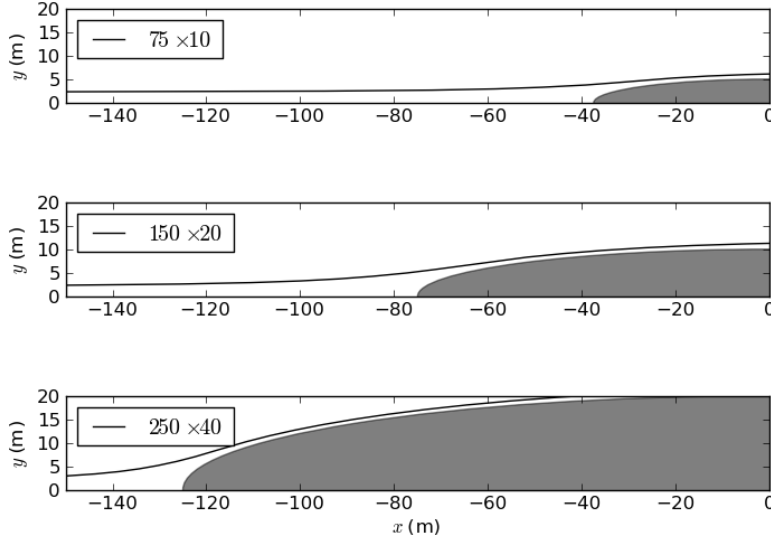
Figure 6 shows histograms of observed ship dimensions (length and draught) and sailing speeds and the aspect ratio versus ship length. The averaged ship length appears to be about 130 m. The average of the aspect ratio is equal to $L/B = 6.4$, yielding an average width of about 20 m. From panel d) it follows that the aspect ratio is more or less constant for ships in excess of 50 m, which is by far the majority of ships, see panel a).

Based on the statistical ship data, three ship dimensions $L \times B$ are considered, see Table 1. Using the (potential) flow field, as defined by (10) and (11), and the glider model (12), glider paths are calculated with the initial position at $x = (-\infty, y)$, where y denotes the distance perpendicular to the centre line of the ship, conform (7). For sufficiently small y , the glider will collide with the ship due to inertia, but for larger y the glider will safely pass the ship. For glider paths that do not intersect the hull, the shortest distance from the path to the hull is denoted by d . Only gliders moving along paths for which $d > \delta$ are not damaged by the ship, defining a critical path by $d = \delta$. It is assumed that $\delta = 0.5$ m, which is approximately half the glider's body size.

The mass of the glider is set equal to 50 kg, whereas the added mass is estimated to be another 50 kg. The water density is taken equal to 1030 kg.m^{-3} . Furthermore, it is assumed that the glider is always orientated perpendicular to the flow. While not necessarily true, a pitching moment gives the glider the tendency to do so, in a similar fashion that a flattened pebble orientates itself in a horizontal position when dropped in water. Then, for a cylinder-shaped object (perpendicular to the flow) $C_d \approx 1$, and

Table 1 Ship dimensions and apparent width.

L (m)	B (m)	B' (m)	B'/B
75	10	2.3	0.23
150	20	2.0	0.10
250	40	1.3	0.03

**Fig. 7** Critical paths for three different ship geometries $L \times B = (75, 10), (150, 20), (250, 40)$ m for ship speed of 6 knots. The starboard side of the bow of the ship is shown in gray.

$A \approx 0.2 \text{ m}^2$ for a glider with a body length of about 1.5 meter and a diameter of about 0.2 m.

The critical paths are shown for the three ship geometries, each sailing at a speed of $u_s = 3 \text{ m/s}$ (6 knots), in Figure 7 by the solid lines. The ship's apparent width B' , defined as the twice the distance from the centre line of the ship and the critical path at $x = -\infty$, is listed in Table 1. Note that the apparent width *decreases* with increasing ship width. An empirical fit is given by

$$\frac{B'}{B} = C_0 \exp\left(-\frac{L}{L_0}\right), \quad (13)$$

where the reference length $L_0 = 100 \text{ m}$, and coefficient of proportionality $C_0 \approx 0.48$.

3.4 Results

Based on the data presented in Figure 6, panel c), ψ is calculated assuming a water depth of 20 m, and a minimum keel-clearance for the glider to glider safely under a ship of 5 m. A histogram is shown in Figure 8. The average value of ψ is about 0.45, which means that in almost 1 in 2 instances a collision is avoided because the glider is deep enough.

The specific data for the NS and EW transect, required to calculate the probability of collision for the missions completing either one NS or EW transect, is given in Table 3. With these data, the probabilities for both transects can be calculated, see Table 2. (The rows in this matrix labelled with “NS Monte-Carlo” and “EW Monte-Carlo” are discussed in the next section.)

The results suggest that the conservative approach, *i.e.* $\psi = 1$ and $B = 20$ m, 1 in 14 crossings of the NS transect is fatal. For the EW transect, the odds are more favourable to the glider, 1 in 333 crossings is expected to be fatal. Taking into account further mitigating factors, *i.e.* the glider escaping collision because of gliding underneath the ship or being pushed aside enough due to the displacement hull, 1 in 250 and 1 in 5000 crossings are expected to be fatal for the NS and EW transects, respectively.

At a speed of 0.5 m/s, the glider traverses about 43 km. For the transects defined herein, this amounts to 1 transect a day. A 30-day mission has probabilities to end prematurely of $30 \times 4 \times 10^{-3} = 0.12$ and $30 \times 2 \times 10^{-4} = 6 \times 10^{-3}$ for the NS and EW transects, respectively. For this $(1 - p)^n$ is approximated by $1 - np$, as $p \ll 1$.

Defining risk as the product of probability of some event and the (financial) consequences, it turns out that the risk of maintaining a 30-day mission covering the NS transect amounts to about €12,000, where the unit price of a glider is estimated at €100,000. This figure excludes any price tag for the data on board the glider that are lost with the device. For the EW transect, the figure is about €600. This means that maintaining the NS transect is prohibitively expensive, whereas the EW transect is feasible from a risk calculation point of view.

4 Monte-Carlo simulation

The rudimentary probability calculations presented in the previous section inevitably required many simplifications and averaging. As a check, this section presents the results of a Monte-Carlo simulation of the same process. A large number of (virtual) gliders, 10,000, say, is deployed at random along a given transect and set off heading for a randomly chosen waypoint. The gliders are scheduled to run for the same period as ship data are collected, but are taken out of service after a collision is detected with a ship.

4.1 Algorithm

Each glider is modelled as a point that moves back and forth between two waypoints at a constant horizontal speed. Both the initial location and heading are set randomly.

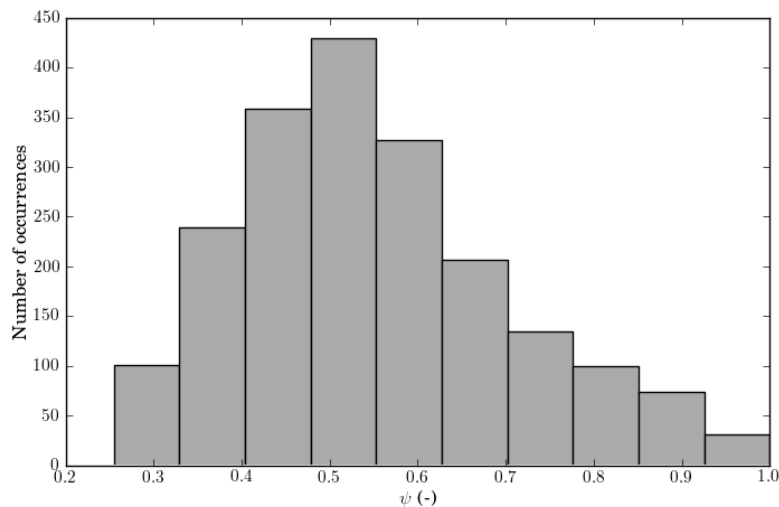


Fig. 8 Histogram of ψ assuming a safe passing for gliders at depth of excess of 5 metres below the hull, and a typical waterdepth of 20 m.

Furthermore, each glider moves in an undulating fashion. A real glider would be programmed such that it would deflect about 2 m above the seabed. Therefore the time required to complete one dive-climb cycle depends on the depth. For reasons of computational efficiency, the dive-climb cycle interval time is set constant, corresponding to a diving depth of 20 m at a vertical speed of 0.2 m/s. This approach allows the glider depth to be calculated directly for any given time since deployment at the expense of a vertical glider speed proportional to the local water depth. As this approach does not bias the glider depth, the results of the Monte-Carlo simulation are not expected to be statistically different.

Whereas the glider positions are calculated, the ship positions are deduced from observed ship motions. To that end, the ship GPS positions are extracted from the AIS data. Subsequently, each ship's specific sequence of GPS positions is split into tracks, where a time interval of two subsequent GPS positions exceeding 2 hours marks a new track. Then, for discrete times with a 30 minutes interval, a pre-selection is made of ships that cross the glider transect during a (centred) time window equal to the time stepping interval. Only these ships may be on a potential collision course with any of the deployed gliders. All pre-selected ships are subjected to a collision detection algorithm, yielding a collision or not.

The detection algorithm models the plan view of a ship as an ellipse, of which the transverse and conjugate radii correspond to half the ship's length and width, respectively, see Figure 9. For a given time window, a function is defined that returns the value of $R - R_s$, where R is the distance between the ship's centre and the position of the glider, and R_s is the radius of the ship's model hull, *i.e.* the ellipse, in the

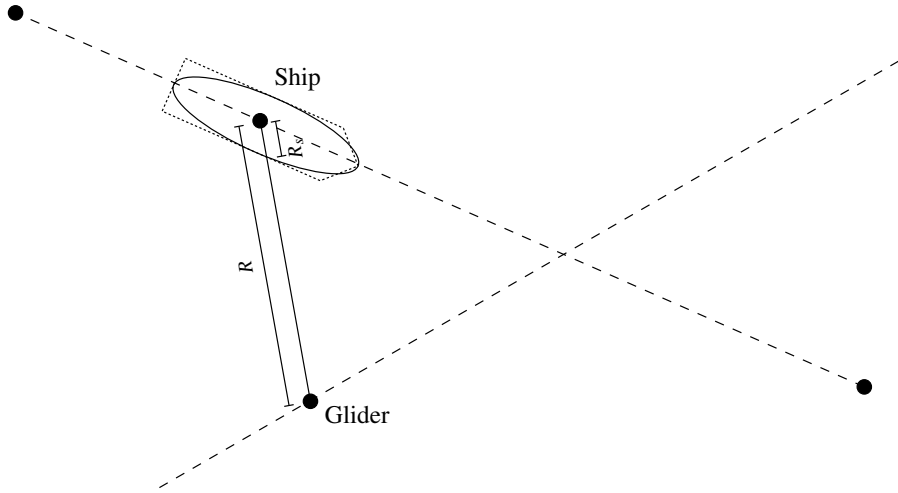


Fig. 9 Schematic representation of the collision algorithm for ship and glider.

direction of the glider, see Figure 9. Subsequently, a search method is applied to find the minimum value of this function. If $R - R_s < 0$ then the glider is within the ship's hull or underneath it. If gliders are not allowed to pass safely underneath a ship a collision occurs, otherwise, a collision is flagged only if the glider's depth is less than the actual ship's draught augmented by a safety margin, set at 5 m. Each collision causes the glider to be taken out of service.

4.2 Results

The probability of a glider loss during a mission can be estimated from the Monte-Carlo simulation results by dividing the size of the population of lost gliders, N , by the size of the initial fleet, N_0 . In the previous section the probability of a glider loss was estimated on a per transect basis. To facilitate the comparison between the two methods, the probability of a glider loss during a mission is calculated from repeated transect crossings,

The (relative) growth of the population of lost gliders as function of the number of completed crossings T is given as a geometrical series

$$N/N_0 = p \sum_{i=0}^{T-1} (1 - p_t)^i = 1 - (1 - p_t)^T, \quad (14)$$

in which p_t is the (constant) probability of collision during a transect crossing, see Table 2. Using the substitution $T = v_g t / L_t$, where t is the time elapsed since deployment, we get

$$N/N_0 = 1 - (1 - p_t)^{\frac{v_g t}{L_t}}. \quad (15)$$

Monte-Carlo simulations were run with virtual glider pools consisting of $N_0 = 10,000$ gliders, deployed along the NS and EW transects described above (and shown in Figure 3). The Monte-Carlo simulation were run for the ship data collected for July 2010. The number of lost gliders, normalised by the number of deployed gliders, is, for four different scenarios (see Table 2), shown in Figure 10 by the solid lines. These results are an estimate for the probability of glider loss as function of deployment duration. The dashed lines represent the theoretical normalised population of lost gliders for constant probability of collision during a single transect crossing, p_t , according to (15), fitted to the Monte-Carlo results.

The results show that the growth of the population of collided gliders progresses in accordance with the theoretical curve calculated from (15). Furthermore, as expected from the results of the previous section, *i*) the probability of collision is substantially higher for the NS section in comparison with the EW section, and *ii*) both reduced ship widths and safe passage underneath ships decrease the probability of collision. The Monte-Carlo results can be compared with the results of the previous section, by comparison of the constant probabilities p_t . The values of p_t found by fitting to the Monte-Carlo results are listed in Table 2, labeled by the rows {NS,EW} Monte-Carlo. The comparison shows that probabilities estimated by the two methods for NS transect differ by less than 20%. The correspondence for the EW transect is not as good; the Monte-Carlo results suggest lower probabilities by a factor of about 2. The poorer comparison may be due to the substantially less intense shipping traffic crossing the EW transect and consequently, the one month of shipping data is statistically less significant for the EW transect compared to the NS transect.

5 Conclusions

Along many coasts and inland waterways, stations are set up for receiving AIS signals. These AIS signals are emitted by most larger ships, and contain information about their position in latitude and longitude, time of position, heading and speed, amongst other things. Collecting this information during a given time frame and area allows to reconstruct the ship tracks. Projecting these tracks onto a grid gives an estimate of the spatial distribution of ship density.

In this work, data were collected for the German Bight for the month July 2010 at 5 minute intervals. The data were then aggregated into chunks of 30 minute intervals. The spatial ship density distribution was estimated for a 1×1 km² grid.

A simple model was formulated to estimate the probability of a collision between a glider and a ship, based on averaged values of ship density and ship dimensions. The formulation (1) shows that, after substitution from $T_t = L_t/v_g$, the probability of a collision during the crossing of a cell is inverse proportional to the glider speed. From this it follows that the probability of a collision *per unit time* is independent of the glider speed.

In addition of the simple probability model formulation, a Monte-Carlo simulation was set up to compare the probability estimates with the prospects of survival of large fleet ($N_0 = 10,000$) of gliders flying amidst a more or less realistic pool of ships of various sorts.

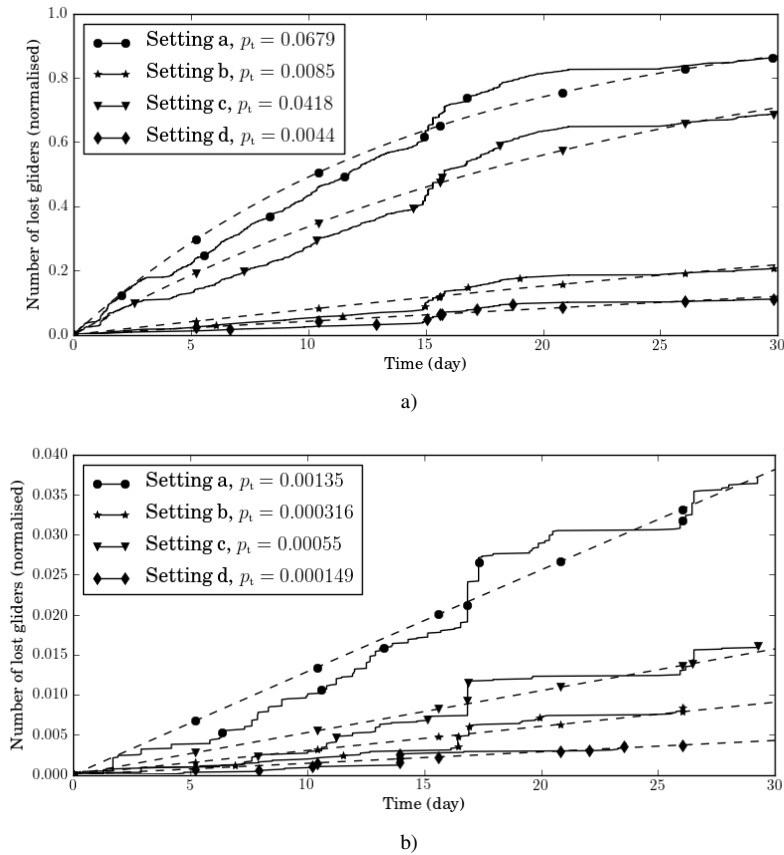


Fig. 10 Results of Monte-Carlo simulations (solid lines) and theoretical populations (dashed lines) for four scenario's, see Table 2. Shown is the relative size of the population of collided gliders, and is an estimate for the probability of glider loss with time. Panel a) and b) show the results for the NS transect and EW transect, respectively.

Because most ships are displacement hulls, objects that are in the path of a moving ship, may be displaced with the water far enough aside so that a collision does not occur. In this study a ship's hull (plan view) was modelled as an ellipse and the flow around the ship as potential flow. It was found that for a cylindrical object corresponding to the size of a glider, the apparent width of a ship is about 1-2 m, which reduces the estimated probability of collision by a factor of 5-20. Estimated probabilities of collision may improve even more by considering that, if flying deep enough, a glider may avoid a collision by crossing underneath a ship. Adopting a safety margin of 5 m underneath the hull, it appears that on average the glider escapes from about 45% of the would-be collisions.

Both models were applied to the data set collected for the German Bight. Two scenarios were considered with transects each of about 40 km, originating from Hel-

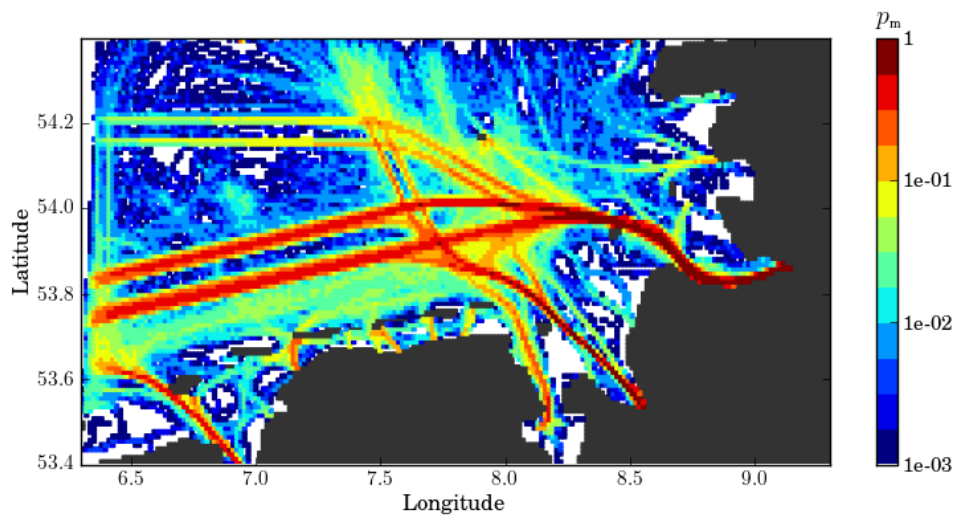


Fig. 11 Map of probability of collision for a residence time of 30 days.

goland, one due South, crossing a busy shipping lane and one due East. Both models were seen to agree for four settings: with or without apparent width, and with or without allowing safe passing underneath ships.

Results show that for a typical mission of 30 days crossing the busy shipping lane (NS transect) the probability of losing a glider is at best 1 in 10 and at worst 8 in 10. The risk for such a mission then amounts to approximately € 50,000, which is prohibitively high. The prospects of glider survival during a 30 day mission along the EW transect are much better. A fairly conservative estimate of glider loss is about 1 in 70, amounting to a risk of € 1500, which seems acceptable.

A synoptic map for the German Bight is shown in Figure 11, in which the probability of collision is shown assuming the glider resides in the same grid cell for 30 days. This map identifies areas with high and low probabilities of ship-glider collisions. Such a map can serve as a useful aid in planning glider transects as well as estimating the risks of a proposed transect or mission.

In conclusion, the simple probability model, discussed herein provides a method for quick estimation of the probabilities involved when flying a glider in busy coastal areas. The method uses the information of AIS signals emitted by ships. Computationally expensive Monte-Carlo simulations were seen to yield results comparable to those of the simple probability model, and are thus not required.

Acknowledgements The author greatly appreciates the permission granted by D. Lekkas from the Department of Product and Systems Design Engineering, University of the Aegean, Greece, to use in this study the data on the ship positions, as obtained from the website <http://www.marinetraffic.com/ais>.

References

1. Davis, R., Eriksen, C., Jones, C.: Autonomous buoyancy-driven underwater gliders. In: G. Griffiths (ed.) *The Technology and Applications of Autonomous Underwater Vehicles*, p. 324. Taylor and Francis, London (2002)
2. Fuji, Y., Shiobara, R.: The analysis of traffic accidents. *Journal of Navigation* **24**(4), 534–543 (1971)
3. Gallos, L., P.Argyrakis: Accurate estimation of the survival probability for trapping in two dimensions. *Physical Review E* **64**, 1–6 (2001)
4. Goerlandt, F., Kujala, P.: Traffic simulation based ship collision probability modeling. *Reliability Engineering and Systems Safety* **96**, 91–107 (2011)
5. Kraus, S.: Rates and potential causes of mortality in north atlantic right whales *Eubalaena Glacialis*. *Marine Mammal Science* **6**(4), 278–291 (1990)
6. Kundu, P.: *Fluid Mechanics*. Academic Press, Inc. (1990)
7. Laist, D., A.R.Knowlton, J.G.Mead, Collet, A., Podesta, M.: Collisions between ships and whales. *Marine Mammal Science* **17**(1), 35–75 (2001)
8. MacDuff, T.: The probability of vessel collisions. *Ocean Industry* pp. 144–148 (1974)
9. Montewka, J., Hinz, T., Kujala, P., Matusiak, J.: Probability modelling of vessel collisions. *Reliability Engineering and Systems Safety* **95**, 573–589 (2010)
10. Mou, J.M., van der Tak, C., Ligteringen, H.: Study on collision avoidance in busy waterways by using ais data. *Ocean Engineering* **37**, 483–490 (2010)
11. Testor, P., Meyers, G., Pattiaratchi, C., Bachmayer, R., Hayes, D., Pouliquen, S., de la Villeon, L.P., Carval, T., Ganachaud, A., Gourdeau, L., Mortier, L., Claustre, H., Taillandier, V., Lherminier, P., Terre, T., Visbeck, Krahman, G., Karstensen, J., Alvarez, A., Rixen, M., Poulain, P., Osterhus, S., Tintore, J., Ruiz, S., Garau, B., Smeed, D., Griffiths, G., Merckelbach, L., Sherwin, T., Schmid, C., Barth, J., Schofield, O., Glenn, S., Kohut, J., Perry, M., Eriksen, C., Send, U., Davis, R., Rudnick, D., Sherman, J., Jones, C., Webb, D., Lee, C., Owens, B., Fratanton, D.: Gliders as a component of future observing systems. In: J. Hall, D. Harrison, D. Stammer (eds.) *OceanObs09: Sustained Ocean Observations and Information for Society, OceansObs'09*, vol. 2. Venice, Italy (2010). ESA Publication WPP-306
12. Vanderlaan, A.: Vessel collisions with whales: the probability of lethal injury based on vessel speed. *Marine Mammal Science* **23**(1), 133–156 (2007)

Table 2 Probabilities of collision per transect, p_t , for the NS and EW transects for various settings.

	setting a $\psi = 1$ $B = 20$ m	setting b $\psi = 1$ $B = 2.6$ m	setting c $\psi = 0.55$ $B = 20$ m	setting d $\psi = 0.55$ $B = 2.6$ m
NS	7.3×10^{-2}	9.6×10^{-3}	4.0×10^{-2}	5.2×10^{-3}
NS Monte-Carlo	6.8×10^{-2}	8.5×10^{-3}	4.2×10^{-2}	4.4×10^{-3}
EW	3.1×10^{-3}	4.0×10^{-4}	1.7×10^{-3}	2.2×10^{-4}
EW Monte-Carlo	1.4×10^{-3}	3.2×10^{-4}	5.5×10^{-4}	1.5×10^{-4}

Table 3 Data specific for the NS and EW transects.

Transect	$\bar{\rho}_s$ (ships per cell per hour)	ψ (-)	T_t (hour)	L_t (m)	n (per transect)
NS	0.160	0.55	0.61	1089	42
EW	0.007	0.55	0.56	1000	40